SAJSET
ISSN: 2992-3581

Savannah Journal of Science and Engineering Technology
Volume: 03; Issue: 01; Pages: 014-024; 2025.
www.sajsetjournal.com.ng

DOI: xx.xxxx.x/sajset-03-2025-0001

SAJSET
ISSN: 2992-3581

Optimization of Nigerian zircon sand partial decomposition using response surface methodology for foundry applications

[1]Kefas H. M., [1]Chiroma T. M., [1]Patrick, D. O. and [1]Mohammed, A.
[1]Chemical Engineering Department, Modibbo Adama University, Yola, Nigeria

Paper History
Received: 24th Dec., 2024
Accepted: 10th Jan., 2025
Published: January, 2025

Abstract:
The purification of zircon sand for industrial applications, particularly in the foundry industry, requires the removal of impurities such as Fe, Al, U, and Th to meet stringent quality and safety standards. Nigerian zircon sands, often sourced from cassiterite tailings, pose challenges due to their high impurity levels, including radioactive elements. This study aimed to optimize the partial decomposition process to enhance the reactivity of Nigerian zircon sands for subsequent acid treatments while avoiding fine milling, which is costly and poses health risks from radioactive dust. A sub-stoichiometric amount of NaOH was used to selectively decompose the metamict regions of zircon, exploiting their higher chemical reactivity. Optimization using Response Surface Methodology (RSM) with Central Composite Design (CCD) determined optimal conditions of 409°C, 49 minutes reaction time, and 0.8 times the stoichiometric NaOH. Under these conditions, significant decomposition of the metamict regions was achieved. XRD analysis revealed a reduction in zircon content from 89% to 75%, monazite from 5% to 1%, and quartz from 3% to 1%, along with the formation of 20% sodium zirconate, indicating successful partial decomposition. XRF analysis confirmed the reduction of impurities, including Fe, Al, U, and Th, while SEM imaging showed the elimination of surface contaminants. Particle size analysis indicated a slight reduction from 218 µm to 214 µm, demonstrating that the process achieved significant chemical changes without substantial physical alteration of the sand. These findings highlight an effective and practical approach for preparing Nigerian zircon sand to meet foundry industry requirements.

Corresponding author
Kefas, H. M.
hmkefas@mau.edu.ng

Keywords: *Alkali fusion, Foundry sand, Metamictization, Optimization, Riruwai zircon*

1. Introduction

Zircon, or zirconium silicate ($ZrSiO_4$), is among the most valuable materials used in the foundry industry. It offers several advantages over other casting sands, such as silica (SiO_2), olivine [$(MgFe)O{\cdot}SiO_2$], and chromite ($FeCr_2O_4$) [1, 2]. Unlike silica, which undergoes phase transformations at elevated temperatures that cause sudden volume changes, zircon remains stable due to its low thermal expansion, making it more suitable for high-temperature environments. Other notable properties of zircon include its high refractoriness, excellent thermal conductivity, superior strength, and reduced tendency to adhere to casting surfaces [3]. Zircon is typically mined alongside other heavy mineral sands, such as ilmenite ($FeTiO_3$), leucoxene ($FeTiO_3{\cdot}TiO_2$), rutile (TiO_2), and monazite [(Ce, La, Th, Nd, Y)PO4]. It can also be recovered from cassiterite (tin) tailings, which represent its primary source in Nigeria [4, 5].

Pure zircon is primarily composed of zirconia (ZrO_2) and silica (SiO_2), which account for approximately 67% and 33%, respectively. However, these proportions may vary due to the presence of impurities such as Fe, Al, P, Ti, U, Th, and rare earth elements (REEs). For foundry applications, zircon must meet stringent quality standards, including a minimum of 65% ZrO_2, a maximum of 32.5% SiO_2, 0.30% Fe_2O_3, 1.5% Al_2O_3, and a combined U and Th content below 500 ppm [6]. However, Nigerian zircon sands are known for their significant impurity levels, particularly uranium and thorium, which can exceed 20,000 ppm [7], far exceeding industrial safety limits. These high impurity levels contribute to their low valuation domestically and internationally [8, 9].

The elevated impurities in some Nigerian zircon sands may result from metamictisation, a process in which radioactive elements decay and create dislocations and vacancies which disrupts the ordered crystal structure of the sand. As the radiation damage progresses, the zircon structure transitions from crystalline to partially or fully amorphous forming metamicts. Metamictisation is known to affect several key physical properties of zircon, such as density, crystallinity, hardness and thermal stability which are all lower compared to crystalline zircon [10]. Additionally, metamict zircon is more chemically reactive because of the disrupted lattice, making it more susceptible to leaching and other chemical treatments. The increased reactivity of metamict zircon can complicate purification

processes, often requiring more extensive chemical treatments to remove impurities. The amorphous regions may also contain higher concentrations of impurities such as Fe, in addition to radioactive elements, posing challenges for handling and disposal [11]. In foundry applications, the altered properties of metamict zircon must be carefully considered, as they may affect the performance of zircon in high-temperature environments where stability and reactivity are critical.

Physical beneficiation methods such as gravity, magnetic, and electrostatic separation, as well as froth flotation, have limitations in removing zircon impurities. Consequently, chemical beneficiation is often required. Common chemical methods include alkali fusion, which decomposes zircon to yield ZrO_2, and acid baking/leaching, which preserves the zircon structure [12]. During alkali fusion zircon reacts with NaOH according to the following reaction:

$$ZrSiO_4 + 4NaOH \rightarrow Na_2ZrO_3 + Na_2SiO_3 + 2H_2O \quad (1)$$

The extent of decomposition in this reaction depends on the amount of NaOH used. Studies indicate that excess NaOH, typically 1.5 times the stoichiometric requirement, at temperatures around 600°C, achieves complete decomposition. Studies have equally shown that varying the amount of NaOH (0.5 – 1.5 times the stoichiometric amount) and temperatures less than 600°C can lead to partial zircon decomposition [13]. For clarity, these ratios will be referred to as the multiplying factor (MF) in this study.

Efforts to purify Nigerian zircon sands have been limited, leaving them undervalued and underutilized. Cassiterite tailings containing zircon are often abandoned at mining sites, representing economic losses and environmental and health risks due to their radioactive content [8, 9]. Conventional methods, which often involve high treatment temperatures (>1200°C) or fine milling, are either unsuitable for altered zircon or economically unfeasible. Fine milling is particularly expensive due to zircon's hardness (Mohs scale: ~7.5) and poses health risks from radioactive dust inhalation more so when the content of radioactive material exceed 1000 ppm [6]. Additionally, methods successful elsewhere have proven ineffective for Nigerian zircon sands, underscoring the need for tailored purification approaches [7].

This study aims to develop a purification method specifically for Nigerian zircon sands, avoiding fine milling and high treatment temperatures. Leveraging the increased chemical reactivity of metamict zircon, a two-stage treatment process is proposed. The first stage involves the selective decomposition of metamict regions using NaOH, followed by a second stage of acid treatment. This paper focuses on optimizing the partial decomposition stage; with process conditions optimized using Response Surface Methodology (RSM).

RSM with Central Composite Design (RSM-CCD) enables the estimation of second-degree polynomials to model the relationships between independent and dependent variables while revealing interactions between variables [14]. RSM was chosen for its efficiency in handling multiple variables and interactions, requiring fewer experiments than traditional one-factor-at-a-time (OFAT) methods. This approach is both cost-effective and time-efficient, facilitating the optimization of experimental conditions for the partial decomposition stage.

2. Methodology

2.1 Materials

The zircon sand used in this study was sourced from physically beneficiated cassiterite tailings from Riruwai, a mining community in Doguwa Local Government Area of Kano State. The beneficiation process included both gravity and magnetic separation. Sodium hydroxide (NaOH) pellets with 99.5% purity, supplied by Sigma Aldrich, along with borax, were utilized as received without further purification.

2.2 Analytical methods

A series of analyses were conducted to characterize the zircon sand before and after partial decomposition. Sieve analysis was used to determine the particle size distribution, while mineral phase analysis was performed using X-ray diffraction (XRD). The chemical composition was assessed through X-ray fluorescence (XRF), and scanning electron microscopy (SEM) was employed to examine the morphology of the samples.

2.3 Experimental design and optimization

The experimental factors were selected based on preliminary studies and literature, particularly the work ofBarawy [13], which focused on optimizing conditions for zircon decomposition. They demonstrated that factors such as temperature, reaction time, and NaOH quantity (MF) influence the degree of zircon decomposition. These factors were varied systematically using a full factorial Central Composite Design (CCD), incorporating factorial and axial points to capture linear, quadratic, and interaction effects. The measured responses were the amount of undecomposed zircon and the remaining uranium and thorium (U + Th) content post-treatment. Design-Expert 7.0 software was used for experimental design and optimization, owing to its user-friendly interface. The high and low factor levels used in the design are listed in Table 1, and a total of 20 experimental runs were conducted, comprising factorial, axial, and center points.

Table 1: Conditions for zircon partial decomposition using NaOH

Factor	Symbol	Levels				
		-2	Low (-1)	Center (0)	High (+1)	+2
Temperature (°C)	A	300	350	400	450	500
Time (min)	B	0	20	40	60	80
MF	C	0.25	0.50	0.75	1.00	1.25

Statistical analysis was performed using Analysis of Variance (ANOVA) to evaluate the individual and interactive effects of variables on the responses. Three tests were conducted: the significance of terms, the lack-of-fit test, and the regression model test, all aimed at assessing the model's significance and reliability. The significant factors were ranked based on their F-values or P-values (probability values) at a 95% confidence level. Larger F-values and smaller P-values (Prob. > F) indicate greater significance of the corresponding coefficients. Model terms were deemed significant only when "Prob. > F" was less than 0.05. A selected model should have an insignificant lack of fit; otherwise, it cannot be used to predict the response [15].

The R^2 value measures how much variability in the observed responses is explained by the experimental variables and their interactions. An R^2 value closer to 1 indicates a better fit of the model to the data. Adjusted R^2 quantifies the variation around the mean explained by the model, adjusting for the number of terms included. It decreases if additional terms do not improve the model. Predicted R^2 measures the model's ability to explain variation in new data. For a reliable model, the difference between adjusted R^2 and predicted R^2 should not exceed 0.20. If this condition is not met, non-significant terms should be removed from the model to improve its performance [14]. Lastly, a model can generally be considered reproducible if its coefficient of variance (CV) is not greater than 10% [15] and an adequacy precision ratio greater than 4 which indicates that the developed model can effectively guide the design space [16].

Numerical optimization was performed to identify the best process conditions to maximize impurity removal while minimizing zircon decomposition, with temperature, reaction time, and NaOH quantity (MF) set within their respective ranges.

2.4 Sample preparation

The zircon sand was thoroughly washed to eliminate organic materials, soluble impurities, and contaminants from storage and transportation. This involved soaking the sand in clean water for 15 to 30 minutes, decanting the water along with floating debris, and rinsing until the water ran clear. The sand was then strained, dried in an oven at 105°C for about 3 hours, and monitored until no further weight change occurred. After cooling to room temperature, the sand was weighed to ensure acceptable moisture levels and stored in clean containers to prevent recontamination. Representative samples were taken throughout the study, with preparation done using the paper cone riffle splitting technique developed by Gerlach et al [17]. New crucibles were tempered with borax to prevent material adhesion during heating.

2.5 Experimental procedure

To carry out the Partial decomposition of zircon sand, 20 g of physically beneficiated zircon sand were weighed and mixed with calculated amounts of NaOH, as determined by the experimental design. The amount of NaOH required for each run was calculated based on the stoichiometric amount calculated from equation 1 and adjusted by a factor ranging from 0.5 to 1.0 (MF) as specified in the design. The mixture was heated in a pre-heated muffle furnace, with temperatures and durations set according to the experimental design.

After each heating cycle, the contents of the crucible were allowed to cool and washed multiple times with distilled water to remove water-soluble fractions such as Na_2SiO_3. The pH of the decanted liquid was monitored after each wash, with a neutral pH indicating complete removal of NaOH and soluble silicates. The resulting residue was dried in an oven at 105°C and weighed at regular intervals until a constant weight was achieved. The samples were cooled and stored in airtight containers for further analyses. Sieve analysis, XRF, XRD and SEM analyses were performed on the dried samples, with the results from XRF and XRD entered into the Design-Expert software for analysis and optimization. The optimal partial decomposition conditions were then validated.

3. Results and discussions

3.1 Analysis and optimizations of zircon sand partial decomposition

The experimental conditions alongside actual and predicted values for $ZrSiO_4$ decomposition and U + Th removal are presented in Table 2. Each row represents a unique experimental combination of temperature, reaction time, and factor to multiply the stoichiometric amount (represented as MF). Comparing actual and predicted values for $ZrSiO_4$ and U + Th provided a measure of the model's accuracy. For instance, in Run 1, the actual $ZrSiO_4$ content was 81%, closely matching the predicted value of 82.77%, while the actual U + Th content of 1.96% was nearly identical to the predicted 1.93%. These small deviations, generally below 2%, demonstrate the model's reliability, well within the maximum acceptable error of 10%. Runs 15 to 20 served as replicates to evaluate result consistency and estimate experimental error. For these runs, the actual $ZrSiO_4$ content ranged from 70% to 74%, while the predicted values remained constant at 72.19%. Similarly, actual U + Th values varied between 1.67% and 1.72%, with predicted values converging at 1.70%. Axial points (Runs 9 to 14) extended the factorial range, capturing potential non-linear behaviour. For example, Run 9, conducted at a lower temperature of 325.91°C, achieved a $ZrSiO_4$content of 78% (predicted: 77.47%), with U + Th removal showing similar agreement (actual: 1.97%, predicted: 1.99%).The close agreement between the actual and predicted values can be seen in Figures 1 and 2.

3.1.1 Model selection

To determine the most suitable model for $ZrSiO_4$ decomposition and U + Th removal, sequential model sum of squares and lack of fit tests shown in Tables 3 – 6 were evaluated. The quadratic model was identified as the best fit for both responses.

3.1.2 Analysis of variance (ANOVA)

ANOVA confirmed the quadratic model's significance for $ZrSiO_4$ decomposition and U+Th removal as shown in

Tables 7 and 8. The model for $ZrSiO_4$ showed a highly significant F-value of 40.47 and a p-value below 0.0001, indicating that variations in decomposition were primarily attributable to independent variables.

Table 2: Experimental runs with output responses for partial decomposition of zircon sand

Std	Point Type	A:Temp (°C)	B:Time (min)	C:MF	$ZrSiO_4$ (%)		U + Th (%)	
					Actual	Predicted	Actual	Predicted
1	Fact	350	20	0.5	81	82.77	1.96	1.93
2	Fact	450	20	0.5	65	65.96	1.92	1.94
3	Fact	350	60	0.5	75	73.70	1.94	1.92
4	Fact	450	60	0.5	71	70.39	1.79	1.75
5	Fact	350	20	1	69	70.26	1.81	1.82
6	Fact	450	20	1	48	49.95	1.63	1.64
7	Fact	350	60	1	62	61.69	1.9	1.88
8	Fact	450	60	1	56	54.88	1.45	1.45
9	Axial	325.91	40	0.75	78	77.47	1.97	1.99
10	Axial	484.09	40	0.75	58	57.61	1.64	1.66
11	Axial	400	6.36	0.75	75	71.78	1.84	1.85
12	Axial	400	73.64	0.75	66	68.30	1.69	1.72
13	Axial	400	40	0.33	74	73.82	1.88	1.92
14	Axial	400	40	1.17	51	50.26	1.58	1.58
15	Center	400	40	0.75	74	72.19	1.67	1.70
16	Center	400	40	0.75	71	72.19	1.71	1.70
17	Center	400	40	0.75	73	72.19	1.69	1.70
18	Center	400	40	0.75	70	72.19	1.72	1.70
19	Center	400	40	0.75	73	72.19	1.72	1.70
20	Center	400	40	0.75	72	72.19	1.68	1.70

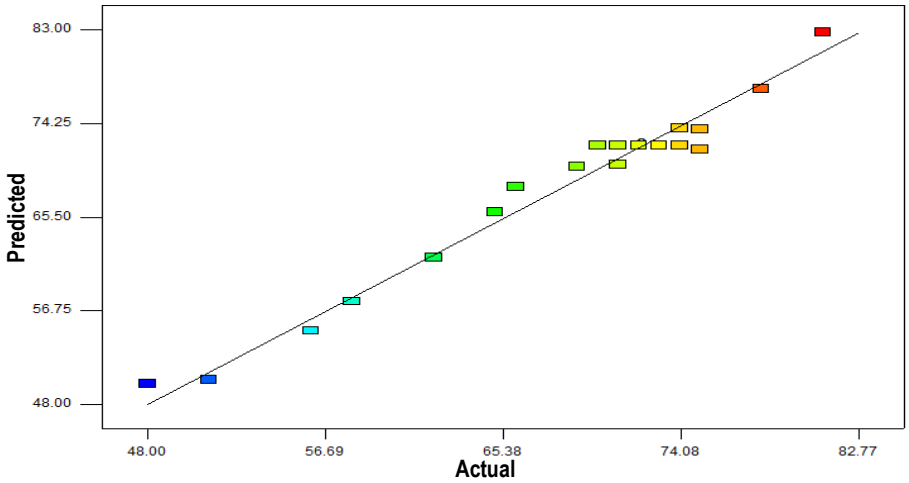

Figure 1: Actual vs predicted values for $ZrSiO_4$ decomposition

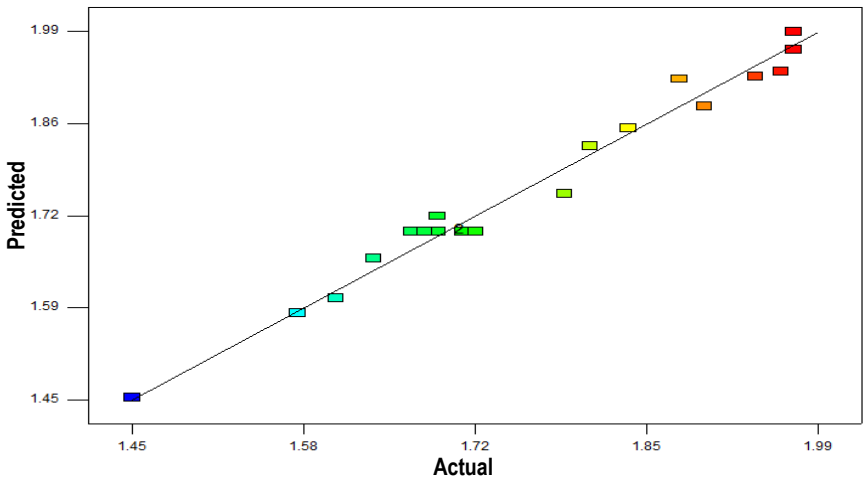

Figure 2: Actual vs predicted values for U + Th removal

Table 3: Sequential model sum of squares for $ZrSiO_4$ partial decomposition

Source	Sum of Squares	df	Mean Square	F Value	p-value Prob> F	
Mean vs Total	92752.20	1	92752.20			
Linear vs Mean	1161.09	3	387.03	16.76	< 0.0001	
2FI vs Linear	97.38	3	32.46	1.68	0.2204	
Quadratic vs 2FI	210.99	3	70.33	17.43	0.0003	Suggested
Cubic vs Quadratic	27.41	4	6.85	3.18	0.1002	Aliased
Residual	12.94	6	2.16			
Total	94262.00	20	4713.10			

Table 4: Lack of fit test for $ZrSiO_4$ partial decomposition

Source	Sum of Squares	df	Mean Square	F Value	p-value Prob> F	
Linear	337.87	11	30.72	14.18	0.0045	
2FI	240.50	8	30.06	13.87	0.0051	
Quadratic	29.51	5	5.90	2.72	0.1478	Suggested
Cubic	2.10	1	2.10	0.97	0.3697	Aliased
Pure Error	10.83	5	2.17			

Table 5: Sequential model sum of squares for U + Th removal

Source	Sum of Squares	df	Mean Square	F Value	p-value Prob> F	
Mean vs Total	62.0224	1	62.0224			
Linear vs Mean	0.2948	3	0.0983	14.98	< 0.0001	
2FI vs Linear	0.0556	3	0.0185	4.89	0.0172	
Quadratic vs 2FI	0.0405	3	0.0135	15.42	0.0004	Suggested
Cubic vs Quadratic	0.0030	4	0.0008	0.79	0.5734	Aliased
Residual	0.0057	6	0.0010			
Total	62.4222	20	3.1211			

Table 6: Lack of Fit Test for U + Th Removal

Source	Sum of Squares	df	Mean Square	F Value	p-value Prob> F	
Linear	0.1027	11	0.0093	20.44	0.0019	
2FI	0.0470	8	0.0059	12.87	0.0060	
Quadratic	0.0065	5	0.0013	2.84	0.1384	Suggested
Cubic	0.0035	1	0.0035	7.59	0.0401	Aliased
Pure Error	0.0023	5	0.0005			

Among the factors, MF had the most substantial influence ($p < 0.0001$, F-value: 166.16), followed by temperature ($p < 0.0001$, F-value: 118.01). Reaction time was less significant ($p = 0.0860$), though it still contributed. Significant interaction effects were observed between temperature and time (AB, $p = 0.0008$, F-value: 22.59), while other interactions, such as temperature and MF (AC) and time and MF (BC), were not significant. Quadratic terms for temperature (A^2, $p = 0.0111$) and MF (C^2, $p < 0.0001$) highlighted non-linear effects, further affirming the quadratic model's suitability. The overall ranking of significance for the model factors are as shown in equation 2:

$$C > A > C^2 > AB > A^2 > B > B^2 > AC > BC \quad (2)$$

The fit statistics further supported the model's validity. For $ZrSiO_4$ decomposition, the R^2value of 0.9733 indicated that 97.33% of the response variability was explained by the model. The adjusted R^2 (0.9492) and predicted R^2 (0.8401) aligned closely, confirming the model's predictive reliability. The adequate precision (Adeq Precision) value of 23.109, well above the threshold of 4, confirms the model's strength.

For U + Th removal, ANOVA results similarly indicated high model significance, with an F-value of 49.57 and p-value < 0.0001. MF and temperature again emerged as the most influential factors, with F-values of 162.47 and 151.13, respectively. Interaction effects (AB and AC) were also significant ($p < 0.001$), suggesting synergistic influences between these factors. In terms of quadratic effects, temperature (A^2), time (B^2), and MF (C^2) were all significant, with F-values of 32.80, 15.32, and 5.41, respectively. This signifies that the non-linear effects of these factors play a role in achieving maximum impurity removal. The overall ranking of significance for the model factors are as shown in equation 3:

$$C > A > AC > A^2 > AB > B > B^2 > C^2 > BC \quad (3)$$

Similarly, the U + Th removal model demonstrated strong predictive accuracy, with R^2= 0.9781, adjusted R^2= 0.9583, and predicted R^2= 0.8651. The lack of fit was insignificant ($p = 0.1384$), demonstrating good agreement between the model and experimental data. Low coefficients of variance (CV) 1.68% further confirmed model reproducibility. Final predictive equations for $ZrSiO_4$ decomposition and U + Th removal are expressed by equations 4 and 5 respectively.

Table 7: ANOVA for response surface quadratic model for $ZrSiO_4$ partial decomposition

Source	Sum of Squares	df	Mean Square	F Value	p-value Prob> F	
Model	1469.46	9	163.27	40.47	< 0.0001	significant
A-Temperature	476.11	1	476.11	118.01	< 0.0001	
B-Time	14.63	1	14.63	3.63	0.0860	
C-MF	670.35	1	670.35	166.16	< 0.0001	
AB	91.13	1	91.13	22.59	0.0008	
AC	6.12	1	6.12	1.52	0.2461	
BC	0.13	1	0.13	0.03	0.8638	
A^2	38.97	1	38.97	9.66	0.0111	
B^2	8.34	1	8.34	2.07	0.1812	
C^2	185.63	1	185.63	46.01	< 0.0001	
Residual	40.34	10	4.03			
Lack of Fit	29.51	5	5.90	2.72	0.1478	not significant
Pure Error	10.83	5	2.17			
Cor Total	1509.80	19				
Std. Dev.	2.01		R-Squared		0.9733	
Mean	68.10		Adj R-Squared		0.9492	
C.V. %	2.95		Pred R-Squared		0.8401	
PRESS	241.44		Adeq Precision		23.1087	

Table 8: ANOVA for response surface quadratic model for U + Th removal

Source	Sum of Squares	df	Mean Square	F Value	p-value Prob> F	
Model	0.3910	9	0.0434	49.57	< 0.0001	significant
A-Temperature	0.1325	1	0.1325	151.13	< 0.0001	
B-Time	0.0200	1	0.0200	22.79	0.0008	
C- MF	0.1424	1	0.1424	162.47	< 0.0001	
AB	0.0210	1	0.0210	23.97	0.0006	
AC	0.0325	1	0.0325	37.10	0.0001	
BC	0.0021	1	0.0021	2.41	0.1516	
A^2	0.0287	1	0.0287	32.80	0.0002	
B^2	0.0134	1	0.0134	15.32	0.0029	
C^2	0.0047	1	0.0047	5.41	0.0423	
Residual	0.0088	10	0.0009			
Lack of Fit	0.0065	5	0.0013	2.84	0.1384	not significant
Pure Error	0.0023	5	0.0005			
Cor Total	0.3998	19				
Std. Dev.	0.030		R-Squared		0.9781	
Mean	1.76		Adj R-Squared		0.9583	
C.V. %	1.68		Pred R-Squared		0.8651	
PRESS	0.054		Adeq Precision		25.6149	

$$ZrSiO_4 = +72.19 - 5.90 * A - 1.04 * B - 7.01 * C + 3.38 * A * B - 0.87 * A * C + 0.13 * B * C - 1.64 * A^2 - 0.76 * B^2 - 3.59 * C^2 \quad (4)$$

$$U + Th = +1.70 - 0.098 * A - 0.038 * B - 0.10 * C - 0.051 * A * B - 0.064 * A * C + 0.016 * B * C + 0.045 * A^2 + 0.031 * B^2 + 0.018 * C^2 \quad (5)$$

Equations 4 and 5 can predict the outcomes of partial decomposition under varying process conditions and guide optimization efforts to enhance impurity removal while preserving $ZrSiO_4$.

3.1.3 Optimization of partial decomposition

To achieve an optimal balance between maximizing $ZrSiO_4$ content and minimizing U and Th levels during the partial decomposition stage, numerical optimization was carried out. The trade-off between the removal of U and Th, which tended to negatively affect $ZrSiO_4$ content, necessitated careful adjustment of process parameters to meet specified targets while adhering to predefined constraints. Table 9 summarizes the optimization criteria, assigned importance of each response, and desirability of the resulting solution.

During the optimization process, greater importance was placed on maximizing $ZrSiO_4$ content to minimize zircon losses during this stage. As the removal of U and Th would be further addressed in the sulfuric acid treatment stage, these impurities were assigned lower importance. The optimal conditions were determined to be a temperature of 408.57°C, a time of 48.99 minutes, and a multiplying factor (MF) of 0.8. Under these conditions, the predicted outcomes were a maximum $ZrSiO_4$ content of 73.99% and a U + Th level of 1.66%. The desirability index for this solution was 0.852, reflecting a satisfactory balance between the competing objectives. A desirability index closer to 1 indicates a more optimal solution [18]. These optimized parameters were subsequently applied to prepare partially decomposed zircon sand for the next stage of treatment. The characterization of actual zircon sand partially decomposed using the optimum conditions are presented in the next section.

Table 9 Numerical optimization for partial decomposition of zircon sand

Constraints Name	Goal	Lower Limit	Upper Limit	Lower Weight	Upper Weight	Importance
Temperature	is in range	350	450	1	1	3
Time	is in range	20	60	1	1	3
MF	is in range	0.5	1	1	1	3
$ZrSiO_4$	maximize	48	81	1	1	5
U + Th	minimize	1.45	1.97	1	1	3
Solutions						
Number	Temperature	Time	MF	$ZrSiO_4$	U + Th	Desirability
1	408.57	48.99	0.8	73.99	1.66	0.852

3.2 Zircon characterization

3.2.1 Zircon particle size

Sieve analysis was conducted on the zircon sand before and after treatment using a standardized method, and the results were analyzed using GRADISTAS package. The findings, presented in Table 10 show that the d_{10} value slightly decreased from 102.1 µm to 99.41 µm, indicating an increase in finer particles. The median size (d_{50}) reduced marginally from 252.2 µm to 246.1 µm, while the d_{90} value remained nearly unchanged at 386.4 µm before treatment and 383.0 µm after decomposition. This suggests that the largest particles were not significantly affected by the NaOH treatment, with fragmentation occurring mainly in smaller particles.

Table 10: Zircon sand sample statistics before and after partial decomposed

Size µm	Physically Beneficiated	Partially Decomposed
d_{10}	102.1	99.41
d_{50} (Median)	252.2	246.10
d_{90}	386.4	383.00
Mean (Geometric)	218.0	214.00

The geometric mean particle size decreased slightly from 218 µm to 214 µm, indicating minimal impact on the bulk particle size. The slight increase in finer particles and the small reduction in median and mean sizes reflect the targeted removal of impurities during NaOH treatment.

The partial decomposition process was conducted at a temperature of 409°C for duration of 49 minutes, with 0.8 times the stoichiometric amount of NaOH required (MF). The results cover the analyses of the chemical composition, mineralogical phases, morphological characteristics, and particle size distribution of the partially decomposed zircon sand.

3.2.2 Mineral phase identification

The mineral phase identification of the physically beneficiated zircon sand, as revealed by X-ray diffraction (XRD), shows that zircon was the dominant phase at 89%, with minor quantities of cassiterite (4%), monazite (5%), and quartz (2%) as shown in Figure 3. The results highlight the limitations of using only physical separation methods to remove gangue minerals from zircon sand. In the case of the partially decomposed sand as shown in Figure 4, zircon remained the dominant phase, although its proportion decreased from 89% to 75%. Though numerical optimization predicted zircon content to be about 74%, the small difference with the actual value is still within the acceptable range. This reduction reflects the partial decomposition of metamict zircon regions, which are enriched with radioactive elements and more susceptible to reaction with NaOH at the optimized conditions used.

A similar partial decomposition was observed by Barawy [13], where about 32% of Egyptian zircon sand decomposed when heated to 400°C for 30 minutes. The higher decomposition in that study can be attributed to the higher NaOH quantity (1.5 times the stoichiometric amount) and smaller zircon sand particle size (63 µm), which increased the surface area for reaction and thus enhances decomposition.

Sodium zirconate (Na_2ZrO_3), a new water-insoluble phase, formed at 20% as a result of the reaction between NaOH and zircon.

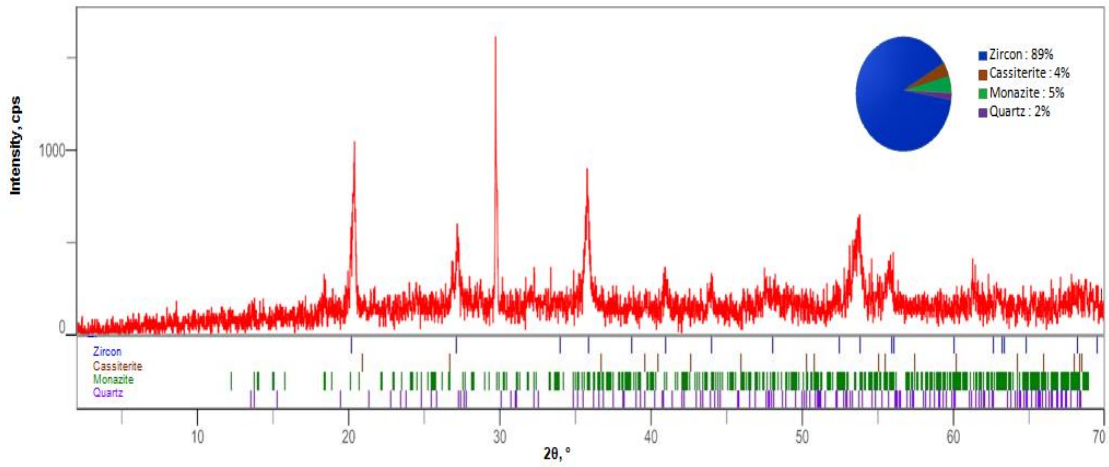

Figure 3 Quantitative XRD analysis of physically beneficiated zircon sand

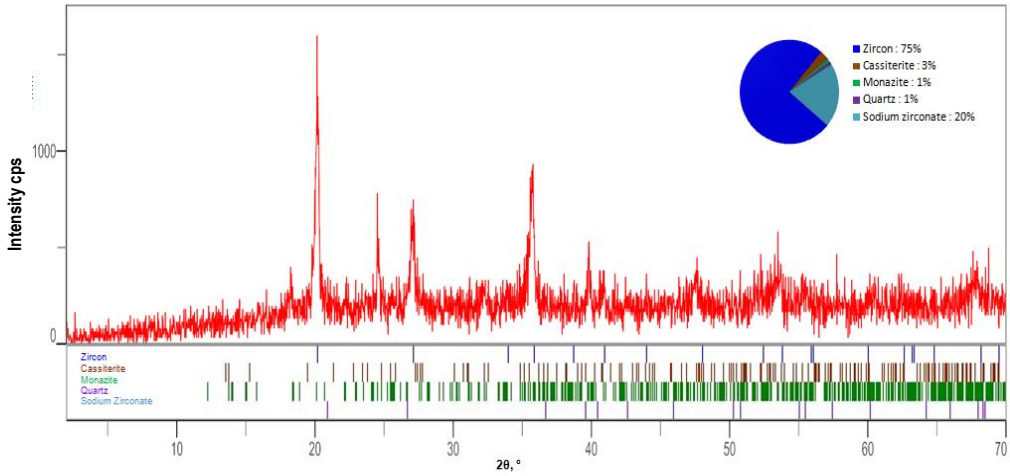

Figure 4 Quantitative XRD analysis of partially decomposed zircon sand

This phase indicates effective targeting of the metamict zones. Sodium zirconate is highly acid-soluble and can be removed in the subsequent purification stage. While the removal of sodium zirconate may lead to zircon losses, it also serves as a precursor for producing zirconium dioxide (ZrO_2), also known as zirconia. Monazite content decreased significantly from 5% to 1%, indicating its high reactivity with NaOH. The decomposition of monazite led to the formation of soluble sodium phosphate, which facilitated the removal of phosphorus and thorium impurities. However, the incomplete removal of monazite may be attributed to its encapsulation within the zircon matrix or insufficient NaOH availability due to the sub-stoichiometric conditions. Quartz content decreased from 2% to 1%, which is consistent with its reaction with NaOH to form soluble sodium silicate (Na_2SiO_3), which was removed during the washing stage. However, the persistence of residual quartz could be due to limited NaOH availability under the sub-stoichiometric conditions, which prevented complete dissolution. Additionally, the encapsulation of quartz within the zircon matrix may have restricted NaOH access.

Cassiterite content showed a slight reduction, from 4% to 3%. Cassiterite is highly resistant to alkali attack [19], which explains its chemical stability under the treatment conditions. The observed reduction may be attributed to mechanical factors, such as cassiterite being physically dislodged during the reaction process. Alternatively, cassiterite may have interacted with impurities, although such reactions are unlikely under sub-stoichiometric NaOH conditions.

3.2.3 Chemical composition of zircon sand

The chemical composition of the physically beneficiated and partially decomposed zircon sand as determined by XRF analyses are presented in Table 11.

The uranium and thorium content of the physically beneficiated zircon sand at 2.62% exceeds the 0.1% (1000 ppm) limit typically associated with the presence of metamict materials [6]. Zambiri [7] similarly reported high impurity levels in zircon sand from cassiterite processing in Bukuru, Plateau State, with Fe_2O_3 at 5.6%, SnO2 at 4.0%, combined U_3O_8 and ThO2 at 2.3%, and HfO_2 at 2.4%. Hafnium content in zircon typically ranges between 1% and 2%, with higher values linked to metamict zircon. Crystalline zircon generally contains around 1.2% HfO_2, while metamict zircon can have up to 3.0%. The Riruwai zircon, with 3.98% HfO_2, indicates the presence of metamict.

Table 11: Chemical composition of zircon sand before and after partial decomposition

Oxide	Concentration (%)	
	Physically Beneficiated	Partially Decomposed
Fe_2O_3	2.88	2.34
SiO_2	27.07	19.71
Al_2O_3	1.87	0.67
P_2O_5	2.06	0.19
Na_2O	- --	4.07
TiO_2	0.46	0.41
CaO	0.35	0.63
PbO	0.20	0.09
ZrO_2	49.10	54.34
ThO_2	1.01	0.61
SnO_2	3.11	2.88
U_3O_8	1.61	1.11
HfO_2	3.98	4.03

Uranium and thorium concentrations in crystalline zircon range from 0.06% to 0.40%, but metamict zircon tends to have higher levels, with uranium typically exceeding thorium [20]. The Riruwai zircon's uranium content of 1.61% and thorium at 1.03% further confirm the presence of metamict material.

The NaOH treatment significantly reduced several impurities, as equally shown in Table 11. The NaOH acted as a fluxing agent, breaking the bonds between zirconium and silica in the zircon matrix. This led to the formation of insoluble sodium zirconate (Na_2ZrO_3) and soluble sodium silicate (Na_2SiO_3), (equation 1) the latter being washed away, reducing SiO_2 from 27.07% to 19.71%. Phosphorus pentoxide (P_2O_5) dropped from 2.06% to 0.19%, and thorium dioxide (ThO_2) from 1.01% to 0.61%, likely due to the decomposition of monazite inclusions. Monazite reacts with NaOH, forming soluble trisodium phosphate (Na_3PO_4) and thorium hydroxide, as seen in equation 6 [21]:

$Th_3(PO_4)_4 + 12NaOH \rightarrow 3Th(OH)_4 + 4Na_3PO_4$(6)

These reductions align with studies [22, 23] which equally showed the effectiveness of NaOH in decomposing monazite-rich sands. Phosphorus removal was more efficient than thorium due to thorium's lower solubility. Uranium oxide (U_3O_8) content decreased from 1.61% to 1.11%, indicating partial removal of radioactive impurities. The lower uranium removal is likely due to its presence in more chemically stable phases within the zircon matrix. Habashi [21] noted similar limitations in uranium removal using alkali treatments, suggesting the need for acid based treatments for further reduction. It can also be observed that combined uranium and thorium in the partially decomposed sand is 1.72%, as against the predicted value of 1.66%, the small difference is still within the acceptable range.

The slight reduction in SnO_2 (from 3.11% to 2.88%) highlights the chemical stability of cassiterite, which is resistant to many acids and alkalis [19]. Aluminium oxide Al_2O_3 decreased from 1.87% to 0.67%, suggesting partial decomposition of aluminous accessory minerals. Iron oxide (Fe_2O_3) content showed a modest reduction, from 2.88% to 2.34%, consistent with iron oxides' limited reactivity with NaOH under these conditions. Da Silva [24] similarly noted limited iron removal during alkali treatments of Brazilian zircon sand, even with excess NaOH at higher temperatures (575°C). The partial reduction in iron content may be due to weak interactions with NaOH via adsorption or surface exchange mechanisms, or physical detachment of iron impurities during the washing step. Zirconia (ZrO_2) content also increased from 49.10% to 54.34%, reflecting successful impurity removal and zirconium concentration. This enrichment is consistent with studies showing increased zirconia concentration through alkaline treatment of zircon sands [11 - 13, 24]. The Na_2O content of 4.07% in the decomposed zircon further confirmed the formation of sodium zirconate.

3.2.4 Morphology of physically beneficiated zircon sand

The scanning electron microscopy (SEM) images of the physically beneficiated and partially decomposed zircon sand are shown in Figures 5 and 6 respectively. Some grains of the physically beneficiated sand exhibit evidence of surface coatings or mineral inclusions as already detected by XRD and XRF analyses.

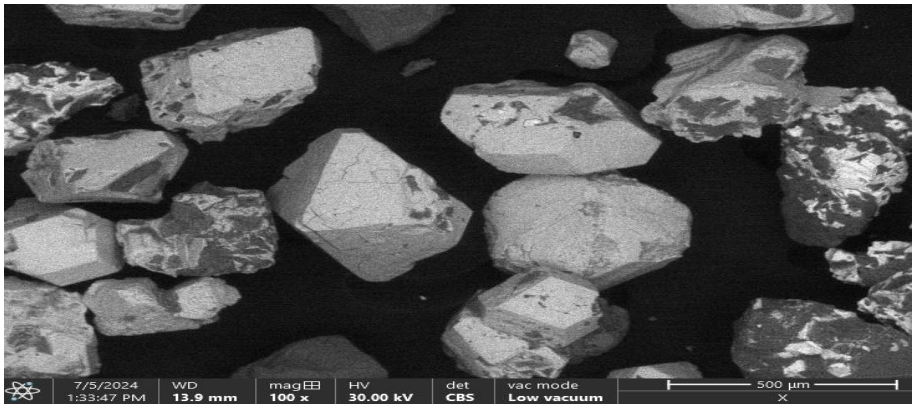

Figure 5: Micrograph of physically beneficiated zircon sand

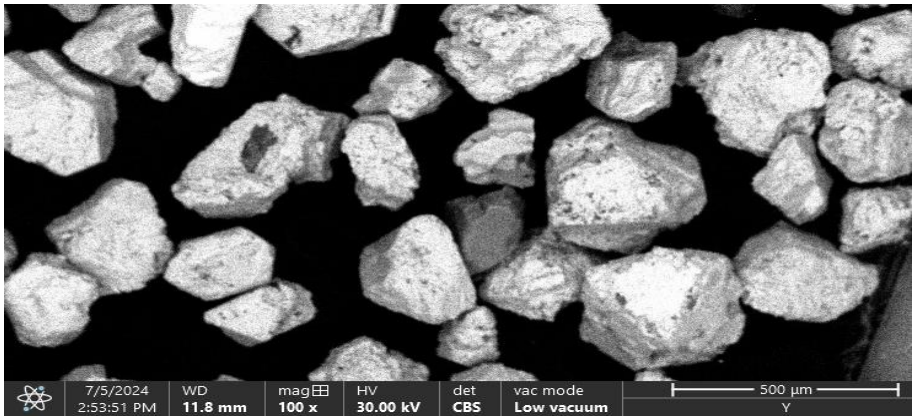

Figure 6: Morphology of partially decomposed zircon sand

The grains also display angular shapes typical of naturally occurring zircon due to its high hardness and resistance to weathering. This angular morphology suggests that the zircon sand has undergone minimal mechanical processing, which is consistent with an untreated sample. The presence of surface cracks and fissures is a prominent feature in the SEM image. These surface defects could be associated with the metamictisation of zircon due to internal radiation damage due to the presence of uranium and thorium. This radiation-induced damage is evident as micro-cracks and fissures on the surface of the grains, which can increase

surface area and create pathways for chemical reagents to penetrate during treatment. Similar micrographs were obtained when zircon concentrates from the Horsham region of Victoria (Australia) which contained metamicts were analyzed [11]. These cracks may enhance the efficiency of impurity removal by providing access to both surface-bound impurities and those within the crystal lattice near the surface. This characteristic can be advantageous during chemical treatments, as the cracks might improve leaching efficiency by exposing more reactive sites. In addition to cracks, the image shows small pits and irregularities on the grain surfaces.

The SEM image of the partially decomposed zircon sand, shown in Figure 6, revealed significant surface modifications, which include etching patterns and fissures, along with the absence of visible surface coatings. Notably, the treated sand displays cleaner surfaces in comparison to the untreated sand, which indicate a significant reduction in impurity layers and exposure of the crystalline zircon surfaces. The changes observed in surface characteristics of the treated zircon sand directly correlate with the results of XRD and XRF analyses, which indicated a reduction in impurity phases after treatment.

4. Conclusion

This study successfully optimized the partial decomposition of Nigerian zircon sand to improve its amenability to subsequent acid treatments. By using a sub-stoichiometric amount of NaOH, the process targeted the selective decomposition of metamict regions, leveraging their increased reactivity. The optimal conditions of 409°C, 49 minutes, and 0.8 times the stoichiometric NaOH effectively decomposed the zircon metamicts. XRD analysis revealed a reduction in zircon content from 89% to 75%, along with decreases in impurities such as monazite and quartz. XRF analysis and SEM imaging confirmed the effective reduction of key impurities, including Fe, Al, U, and Th, while the slight reduction in particle size from 218 to 214 µm suggests minimal physical alteration of the sand structure. The findings demonstrate that the optimized partial decomposition process not only facilitates the subsequent acid treatments but also helps sustainable beneficiation practices by avoiding fine milling and mitigating health risks associated with radioactive dust.

References

[1]. Jain, P.L., (2009). Principles of Foundry Technology, 5th ed. McGraw-Hill Education Private Limited, New Delhi.

[2]. Dunan, C. F. (2019).Technical Handbook on Zirconium and Zirconium Compounds. Zircon Industry Association, Mayfair, London.

[3]. Bansode, S.N., Phalle, V.M. and Mantha, S.S. (2020). Influence of slurry composition on mould properties and shrinkage of investment casting, *Transactions of the Indian Institute of Metals*, 73(3), 763–773.

[4]. Ejiofor, J. U., Okorie, B. A. and Reddy, R. G. (1997). Powder processing and properties of zircon-reinforced Al-13.5Si-2.5Mg alloy composites. *Journal of Materials Engineering and Performance*, 6, 326–334.

[5]. Okoli, B. I., Agboola, O. A., Onwualu, A. P., Bello, A., Sholiyi , O. S., Anye, V. C. and Yusuf, O.T.(2023). Characterization of nigerian zircon sand and its suitability for different industrial applications. *Minerals*, 13(6), 1-26.

[6]. Pownceby, M.I, Sparrow, G.I., Aral, H., Smith, L.K. and Bruckard, W.J. (2015). Recovery and processing of zircon from murray basin mineral sand deposits. *Mineral Processing and Extractive Metallurgy*, 124(4), 240–253.

[7]. Zambiri, S. (2009). Purification of some Nigerian zircon for use as opacifier using ammonium sulphate. Unpublished master's thesis. Modibbo Adama University, Yola.

[8]. Funtua, I. I. and Elegba, S. B., (2007). *Radiological assessment of zircon processing in Nigeria*. The Fifth International Symposium on Naturally Occurring Radioactive Material, Seville, 117–119.

[9]. Muhammad, A. M., Funtua, I. I., Dewu, B. B. M. and Mallam, S. P., (2013). *Radioactivity in Zircon from Jos, Central Nigeria*. The Seventh International Symposium on Naturally Occurring Radioactive Material, Beijing, 639–643.

[10]. Smith, M. J., Jones, E., Blackburn, S. and Greenwood, R. W. (2023). Understanding the effect of metamictisation on the efficiency of zircon milling, *Minerals Engineering*, 197, 108065.

[11]. Aral, H., Sparrow, G. J., Mcdonald, K. and Norgate, T. E. (2007). Pure zircon process for removing radionuclides from zircon concentrates. *Transactions of the Institute of Mining and Metallurgy*, 116(3), 145–151.

[12]. Subuki, I., Norsham, N. F. F., Mahayuddin, N. A. and Ali, Q. M. (2022). Influence on ratio of NaOH /$ZrSiO_4$ in alkali fusion for Amang zircon sand. *ASM Science Journal*, 17, 1–10.

[13]. Barawy, K. A., El Tawil, S. Z. and Francis, A. A. (2000). Alkali fusion of zircon sand, *Mineral Processing and Extractive Metallurgy*, 109(1), 49–56.

[14]. Taran, M. and Aghaie, E. (2015). Designing and optimization of separation process of iron impurities from kaolin by oxalic acid in bench-scale stirred-tank reactor, *Applied Clay Science*, 107, 109–116.

[15]. Wang, X., Xiang, J., Pei, G., Li, L., Huang, Q. and Lu, X. (2021). Application of response surface methodology for roasting optimization in composite roasting—acid leaching vanadium extraction process, *Chemical Engineering Research and Design*, 172, 254–263.

[16]. Behera, S. K., Meena, H., Chakraborty, S. and Meikap, B. C. (2018). Application of response surface methodology (RSM) for optimization of leaching parameters for ash reduction from low-grade coal, *International Journal of Mining Science and Technology*, 28(4), 621–629.

[17]. Gerlach, R. W., Dobb, D. E., Raab, G. A. and Nocerino, J. M. (2002). Gy sampling theory in

environmental studies: assessing soil splitting protocols, *Journal of Chemometrics*, 16, 321–328.

[18]. Kraber, S. (2023). Unraveling the Mystery of Multi-Response Optimization. https://www.statease.com/blog/unraveling-the-mystery-of-multi-response-optimization/

[19]. Tapster, S. and Bright, J. W. G. (2020). High-precision ID-TIMS cassiterite U–Pb systematics using a low-contamination hydrothermal decomposition: implications for LA-ICP-MS and ore deposit geochronology, *Geochronology*, 2(2), 425–441.

[20]. Zaman, M. and Antao, S. (2020). Crystal chemistry and structural variations for zircon samples from various localities. *Minerals*, 10(11), 947.

[21]. Habashi, F. (2013). Extractive metallurgy of rare earths, *Canadian Metallurgical Quarterly*, 52(3), 224–233.

[22]. Berry, L., Galvin, J., Agarwal, V. and Safarzadeh, M. S. (2017). Alkali pug bake process for the decomposition of monazite concentrates, *Minerals Engineering*, 109, 32–41.

[23]. Udayakumar, S., Baharun, N., Rezan, S. A., Ismail, A. F. and Mohamed Takip, K. (2021). Economic evaluation of thorium oxide production from monazite using alkaline fusion method, *Nuclear Engineering and Technology*, 53(7), 2418–2425.

[24]. Da Silva, R. J. F., Dutra, A. J. B. and Afonso, J. C. (2012). Alkali fusion followed by a two-step leaching of a Brazilian zircon concentrate, *Hydrometallurgy*, 117–118, 93–100.